

# The Na I and Sr II Resonance Lines in Solar Prominences

G. Stellmacher<sup>1</sup> · E. Wiehr<sup>2</sup>

© Springer .....

**Abstract** We estimate the electron density,  $n_e$ , and its spatial variation in quiescent prominences from the observed emission ratio of the resonance lines Na I 5890 Å (D<sub>2</sub>) and Sr II 4078 Å. For a bright prominence ( $\tau_\alpha \approx 25$ ) we obtain a mean  $n_e \approx 2 \times 10^{10} \text{ cm}^{-3}$ ; for a faint one ( $\tau_\alpha \approx 4$ )  $n_e \approx 4 \times 10^{10} \text{ cm}^{-3}$  on two consecutive days with moderate internal fluctuation and no systematic variation with height above the solar limb. The thermal and non-thermal contributions to the line broadening,  $T_{\text{kin}}$  and  $V_{\text{nth}}$ , required to deduce  $n_e$  from the emission ratio Na I/Sr II cannot be unambiguously determined from observed widths of lines from atoms of different mass. The reduced widths,  $\Delta\lambda_D/\lambda_0$ , of Sr II 4078 Å show an excess over those from Na D<sub>2</sub> and Hδ 4101 Å, assuming the same  $T_{\text{kin}}$  and  $V_{\text{nth}}$ . We attribute this excess broadening to higher non-thermal broadening induced by interaction of ions with the prominence magnetic field. This is suggested by the finding of higher macro-shifts of Sr II 4078 Å as compared to those from Na D<sub>2</sub>.

**Keywords:** Prominences, Models; Spectral Line, Broadening

## 1. Introduction

The knowledge of fundamental plasma parameters in solar prominences like electron density,  $n_e$ , and kinetic temperature,  $T_{\text{kin}}$ , is still rather unsatisfactory (*cf.*, Labrosse *et al.*, 2010). The large range of  $n_e$  values may be illustrated by the analysis of Bommier *et al.* (1994), who interpret Hanle-effect observations of H $\alpha$  and HeD<sub>3</sub> and obtain  $0.25 \times 10^{10} \leq n_e \leq 6.3 \times 10^{10} \text{ cm}^{-3}$  with a mean

---

✉ G.S.  
stell@iap.fr  
E.W.  
ewiehr@astro.physik.uni-goettingen.de

<sup>1</sup> Institute d'Astrophysique (IAP), 98 bis Blvd. d'Arago, 75014 Paris, France

<sup>2</sup> Institut f. Astrophysik, Fr.-Hund-Platz 1, 37077 Göttingen, Germany

of  $n_e = 2.1 \times 10^{10} \text{ cm}^{-3}$ . Koutchmy *et al.* (1983) derived from eclipse spectra of  $\text{H}\beta$  and the Balmer continuum  $n_e < 2.5 \times 10^{10} \text{ cm}^{-3}$ .

Landman (1983a) calculated for a homogeneous atmosphere the dependence of the  $\text{NaD}_2$  and  $\text{Sr II } 4078 \text{ \AA}$  emissions on  $n_e$ , and compared (in Landman, 1983b) the ratio of their integrated line emission with observations by Shih-Huei (1961) and by Yakovkin and Zel'dina (1964), deducing a mean electron density  $n_e \approx 6 \times 10^{10} \text{ cm}^{-3}$ . Considering more energy levels of  $\text{Na I}$  and  $\text{Sr II}$ , Landman (1986) revised his 1983 results for  $n_e$  by a factor of 0.5, leading to a mean electron density  $n_e \approx 3 \times 10^{10} \text{ cm}^{-3}$ .

Although Landman (1983a) found only a slight dependence on the line-broadening parameters, these cannot be fully neglected. Thermal and non-thermal contribution to line-broadening,  $T_{\text{kin}}$  and  $V_{\text{nth}}$  cannot unambiguously be obtained from Doppler widths: Balmer, helium and metallic lines do not yield a common pair  $[T_{\text{kin}}, V_{\text{nth}}]$ . Wiehr *et al.* (2013) found that the reduced Doppler widths  $\Delta\lambda_D/\lambda_0$  of lines from ions are generally too broad as compared to those from neutrals.

Such a selective excess broadening cannot occur in a homogeneous prominence plasma, where neutrals and ions behave as in a one-component fluid (Terradas *et al.*, 2015). On the other hand, Low *et al.* (2012) showed that condensations of cool gas must occur in prominences “as a consequence of the non-linear coupling of force balance and energy transport”. This “catastrophic radiative cooling” causes gas clumps to become largely neutral, and their frozen-in state breaks down. These clumps then sink and progressively “warm up by resistive heating” until, at sufficient re-ionization, the clumps are eventually again frozen-in and stop sinking.

If some fraction of this alternating ‘stop-and-go’ falling motion shows up as non-thermal velocity (due to turbulence and/or shocks; *cf.* Hillier *et al.*, 2012), an excess broadening should occur for lines of the (sinking) neutrals. Yet, the observed broader lines from ions (Stellmacher and Wiehr, 2015), supposed to be frozen-in, rather indicate the contrary. We examine this scenario comparing the width of  $\text{Sr II } 4078 \text{ \AA}$  and  $\text{NaD}_2$ , which may probe prominence regions with different excitation conditions.

## 2. Observations

With the Vacuum Tower Telescope, VTT, on Tenerife we observe four quiescent prominences in 2015. Two brighter ones are observed on August 31 (B) and September 1 (C), a medium bright one on August 30 (A) and a fainter one on two successive days on September 2 and 3 (D). Characteristic parameters for these prominences are given in Table 1.

The neighboring lines  $\text{Sr II } 4078 \text{ \AA}$  and  $\text{H}\delta$  are simultaneously recorded in the 55th order and  $\text{NaD}_2$  is recorded in the 38th order about 1 min later after a change of the spectrograph setting, since the pre-selector of the VTT does not allow a simultaneous observation of both lines. The neighboring  $\text{He } 3888 \text{ \AA}$  and  $\text{H}_8 3889 \text{ \AA}$  lines are recorded in the 58th order a further minute later. The CCD exposure is 50 ms and the width of the spectrograph-slit of 0.55 arcsec

corresponds to 400 km on the Sun. We estimate the influence of seeing during the 50 ms exposures to amount to 1.5 arcsec.

**Table 1.** Parameters of the observed prominences: designation, date, limb position, maximum H $\delta$  brightness [erg/(s cm<sup>2</sup> ster)], and the corresponding optical depths taken from the tables by Gouttebroze, Heinzel, Vial (1993)

prominence	date	position	$E^{\max}(\delta)$	$\tau^{\max}(\delta)$	$\tau^{\max}(\alpha)$
A	Aug. 30	E/10S	$13 \cdot 10^3$	0.15	7
B	Aug. 31	E/15S	$25 \cdot 10^3$	0.29	13
C	Sept. 1	W/35N	$46 \cdot 10^3$	0.5	25
D	Sept. 2	W/15S	$8 \cdot 10^3$	0.09	4
D	Sept. 3	W/15S	$8 \cdot 10^3$	0.09	4

Spectra of the (emission free) prominence neighborhood are taken immediately before and after each exposure for a determination of the stray-light aureole (mainly Rayleigh scattering on the mirror surfaces, *cf.*, Stellmacher and Wiehr, 1970). The change of the spectrograph setting between the two exposures (Na D, respectively, Sr II with H $\delta$ ) does not preserve the wavelengths precisely on the CCDs. As a consequence, the aureole exposures have to be repeated for each set of emissions. This, in turn, requires that the telescope be pointed alternately to the prominence and to its neighborhood. Since the VTT occasionally does not return precisely to the same prominence position, we only use those Na D<sub>2</sub> spectra, which visually correlate with the corresponding Sr II and H $\delta$  spectra.

The integrated emissions,  $E_{\text{tot}}$ , are calibrated in absolute units [erg/(s cm<sup>2</sup> ster)] with spectra of the disk center, scaled with values by Labs and Neckels (1970); Ramelli *et. al.* (2012) described the reduction procedure in detail. We determine line profiles in spatial emission maxima averaged over 3 pixels of the 2-pixel binned CCDs, corresponding to  $\approx 1$  arcsec. The estimated seeing of  $\approx 1.5$  arcsec corresponds to a resolution area of 1000 km  $\times$  1000 km on the sun. Different refraction of the yellow Na D and the violet Sr II light is well below 0.5 arcsec at 2400 m above sea level and a solar zenith distance of  $< 35^\circ$ .

The obtained emission line profiles are fitted by Gaussians. The main uncertainty arises from the accuracy of the zero level, which is affected by residual absorption lines from the stray-light aureole. We determine the zero level as broad-band median intensity outside the respective emission line. In order to avoid an influence of line asymmetries we successively fit the upper 10%, 40% and 70% of each emission profile. For the determination of the wavelength position on the CCD, we use only the upper 10%, thus avoiding influences from blending by emission satellites. For a determination of the line widths,  $\Delta\lambda_e$ , and of the integrated line intensity,  $E_{\text{tot}} = \int I_\lambda d\lambda$ , we use only symmetric profiles for which the three Gaussians (of 10%, 40%, 70%) do not significantly differ. In this way we estimate the shift accuracy to be  $\leq 0.5$  pixel, corresponding to  $\Delta V_{\text{macro}} \leq 0.01$  km/s or  $\Delta\lambda_e \leq 2$  mÅ, and  $\Delta E_{\text{tot}}/E_{\text{tot}} \leq 0.05$ .

### 3. Results

For several exposures the visual aspects of the Na D<sub>2</sub> and the Sr II 4078 Å emissions are so conspicuously similar that it is impossible to distinguish them at first glance. This is shown in Figure 1 for a set of spectra of prominence D. We reasonably assume that this similarity is real, and that an occasionally occurring poorer coincidence of both lines is due to imperfect return of the VTT from the intermediate aureole pointing to the precedent location in the prominence, and possibly also to different influence of seeing during the two exposures.

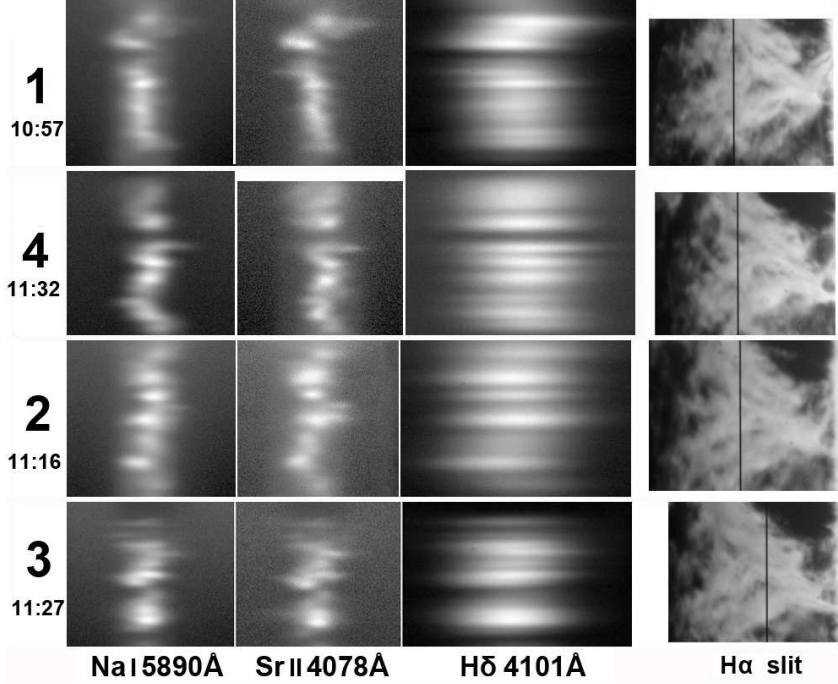


**Figure 1.** Spectra of NaD<sub>2</sub>, Sr II and Hδ for prominence D at slit-positions 1, 4, 2 and 3, decreasing with height above the solar limb (black vertical lines at right border of Hα slit yaw images). Each spectrum covers 0.6 Å × 70 arcsec.

#### 3.1. Total Emission and Electron Density

The ratio of the total line emissions,  $E_{\text{tot}} = \int I_{\lambda} d\lambda$ , of NaD<sub>2</sub> and Sr II 4078 Å allows to estimate the electron density  $n_e$ . Landman (1983a) found that under prominence conditions the Sr atom is mainly ionized. He gave for the Sr II resonance line a Boltzmann distribution with  $n(\text{Sr II}, 5^2P) \approx n(\text{Sr II}) \approx n(\text{Sr}^{\text{tot}})$ , largely independent of temperature. The Na I resonance line can only be emitted after recombination and is thus sensitive to  $n_e$ . Landman (1983) found a Saha-Boltzmann distribution with  $n(\text{Na I}, 3^2P) \propto n_e n(\text{Na II}) \approx n_e n(\text{Na}^{\text{tot}})$ .

Spectra showing a good correlation of NaD<sub>2</sub> and Sr II yield for the prominences A, B and C the mean line emission ratios  $E(\text{Na I})/E(\text{Sr II})$  of 1.6, 1.25

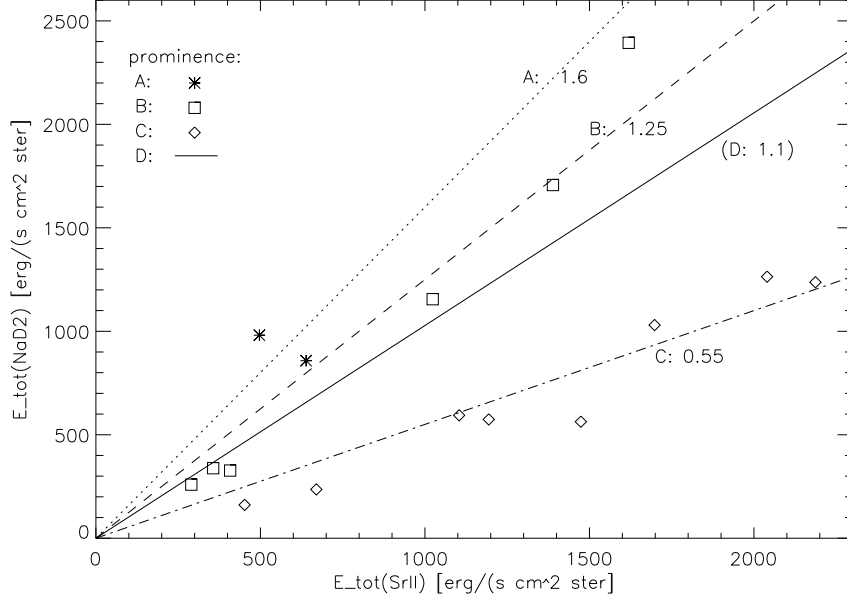


**Figure 2.** Integrated line emission,  $E_{\text{tot}}$ , of Na D<sub>2</sub> and Sr II 4078 Å for prominences A, B and C. Dotted, dashed and dash-dotted lines give the corresponding linear fits; for prominence D we plot the mean slope of 1.1 (thick) from Figure 3.

and 0.55, respectively (see Figure 2). With the relations of Landman (1983a) calculated for kinetic  $T_{\text{kin}} = 8000 \text{ K}$  and non-thermal  $V_{\text{nth}} = 3 \text{ km/s}$  broadening parameters, and their correction following Landman (1986) by a factor of 0.5, we obtain for these ratios mean electron densities of  $n_e = 7, 5$  and  $2 \times 10^{10} \text{ cm}^{-3}$  for prominences A, B and C (Table 2).

Prominence D is observed with an extended coverage of slit-positions and on two successive days. This allows us to study the spatial and temporal variation of the  $E_{\text{tot}}$  ratio and thus of  $n_e$ . Figure 3 shows for September 3 an internal scatter of the ratio with a mean of 1.1 corresponding to  $n_e \approx 4.2 \times 10^{10} \text{ cm}^{-3}$ . We find no systematic dependence on height above the solar limb or on the Balmer brightness  $E_{\text{tot}}(\text{H}\delta)$ . On September 2, the mean emission ratio of 1.0 indicates no marked time variation of  $n_e$  with the prominence evolution over 24 hours.

Although the exact knowledge of  $T_{\text{kin}}$  and  $V_{\text{nth}}$  is of no great importance (Landman 1983a), the systematic ambiguity of these values (see Section 3.2) introduces an uncertainty. Its amount is illustrated by comparison with Landman’s (1983a) calculations for  $T_{\text{kin}} = 5000 \text{ K}$  and  $V_{\text{nth}} = 5 \text{ km/s}$  (brackets in Table 2), which gives about 20% lower  $n_e$  values than calculations for  $T_{\text{kin}} = 8000 \text{ K}$  and  $V_{\text{nth}} = 3 \text{ km/s}$  (see Table 2).

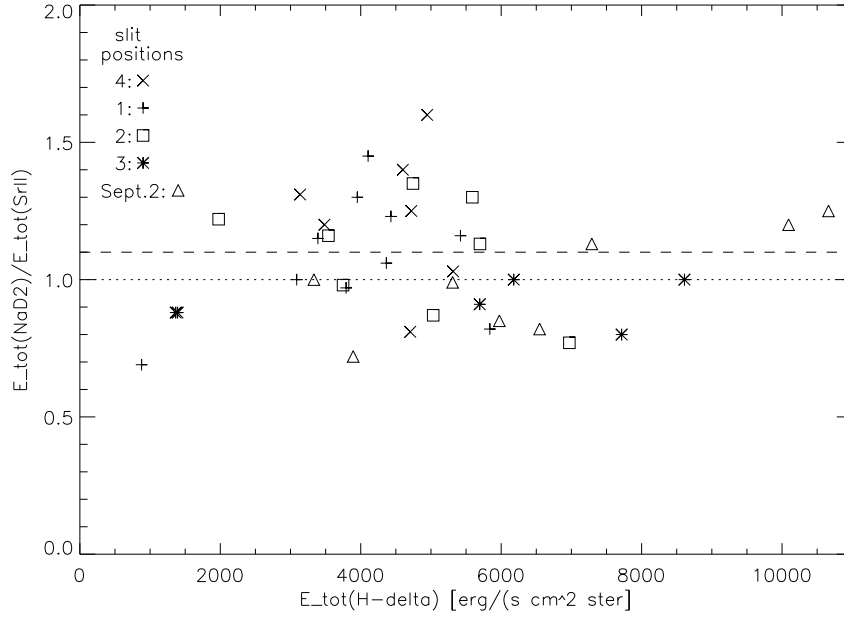


**Figure 3.** Ratio of integrated line emissions  $E_{\text{tot}}(\text{Na D}_2)$  and  $E_{\text{tot}}(\text{Sr II } 4078)$  versus  $E_{\text{tot}}(\text{H}\delta)$  for prominence D on September 3 at 4 slit positions decreasing with height above the limb (see Figure 1), giving a mean of 1.1 (dashed line), and for September 2 with a mean of 1.0 (dotted line).

**Table 2.** Emission ratio of  $\text{Na D}_2$  and  $\text{Sr II } 4078 \text{ \AA}$  and electron density  $n_e [10^{10} \text{ cm}^{-3}]$  deduced from the diagrams by Landman (1983a, 1986) for  $T_{\text{kin}} = 8000 \text{ K}$  and  $V_{\text{nth}} = 3 \text{ km/s}$ ; the values for  $T_{\text{kin}} = 5000 \text{ K}$  and  $V_{\text{nth}} = 5 \text{ km/s}$  are in parentheses; columns 4 and 5 give the reduced Doppler widths  $\Delta\lambda_D/\lambda_0 [10^{-5}]$  of  $\text{Na D}$ ,  $\text{Sr II}$  and  $\text{H}\delta$  for the prominences listed in Table 1.

prominence	date	E (Na/Sr)	$n_e$	width (Na)	width (Sr)	width (H)
A	Aug. 30	1.6	7.0 (5.0)	1.2	1.1	3.8
B	Aug. 31	1.25	5.0 (4.0)	1.63	1.85	4.0
C	Sept. 1	0.55	2.0 (1.7)	1.55	1.82	4.3
D	Sept. 2	1.0	4.0 (3.2)	1.12	1.17	3.68
D	Sept. 3	1.10	4.2 (3.5)	1.1	1.06	3.78

### 3.2. Line Widths

The deduction of the electron density  $n_e$  from the emission ratio depends little on the thermal,  $T_{\text{kin}}$ , and non-thermal,  $V_{\text{nth}}$ , contributions to line-broadening. These parameters are commonly obtained from inter-comparison of Doppler widths,  $\Delta\lambda_D$ , of optically thin lines (*i.e.*, with Gaussian profiles) emitted by atoms of different atomic mass  $\mu$ , following

$$(V_D)^2 = (c\Delta\lambda_D/\lambda_0)^2 = 2RT_{\text{kin}}/\mu + V_{\text{nth}}^2, \quad (1)$$

where  $R$  is the gas-constant and  $V_{\text{nth}}$  is the non-thermal line broadening with a Maxwellian velocity distribution. A necessary condition for the validity of this equation is that the lines originate in the same volume element. Since blending from unresolved macro-velocities introduces additional line-broadening (*e.g.*, Gunár *et al.*, 2008), we determine  $\Delta\lambda_D$  from those spatial emission maxima in the spectra which show symmetric line profiles (*cf.* end of Section 2).

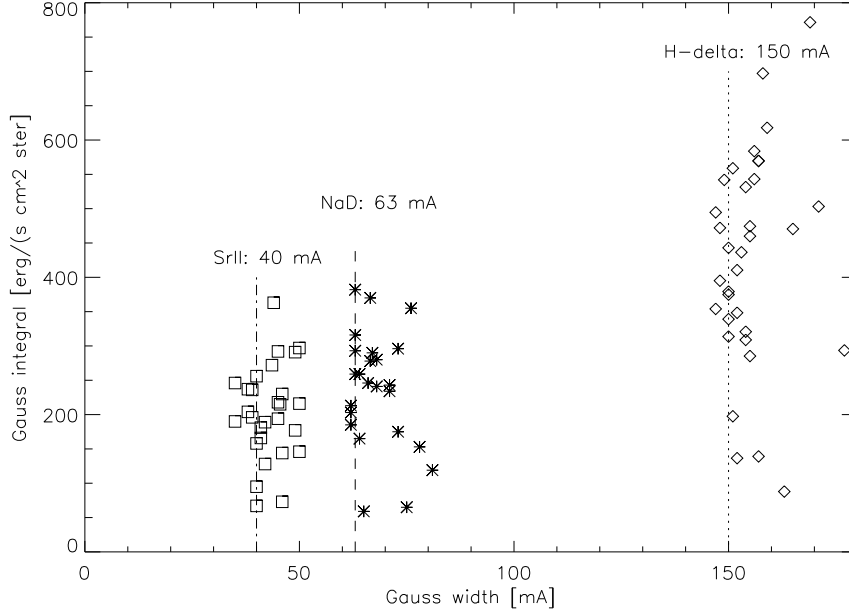


**Figure 4.** Relation of the width  $\Delta\lambda_e$  and the integrated intensity  $E_{\text{tot}}$  of the Gaussian fits of Sr II 4078 (boxes), NaD<sub>2</sub> (asterisks) and H $\delta$  (rhombs; scaled to 1/10) for the spatial emission maxima in the four spectra of prominence D shown in Figure 1. The lower means of  $\Delta\lambda_e$  (vertical lines) are labeled for each emission line with the relevant values, representing the mean  $\Delta\lambda_D$  over the prominence D.

In Figure 4 we plot  $\Delta\lambda_e$  and  $E_{\text{tot}}$  from the Gaussian fits of the three emission lines in all spectra of the well documented prominence D (*cf.* Figure 1). We insert a reasonable lower mean  $\Delta\lambda_e^{\text{mean}}$  (vertical lines) for each emission line, which accounts for additional line broadening (at the right side) and statistical noise (at the left side of each mean). We find no significant dependence of  $\Delta\lambda_e$  on the emission brightness  $E_{\text{tot}}$ .

Assuming Doppler widths  $\Delta\lambda_D = \Delta\lambda_e^{\text{mean}}$ , we obtain for the mostly temperature broadened H $\delta$ ,  $\Delta\lambda_D = 150 \text{ mÅ}$ , which gives, with Equation (1), an upper limit (*i.e.*,  $V_{\text{nth}} = 0$ ) of  $T_{\text{kin}} \leq 7350 \text{ K}$ . The mostly turbulence-broadened Sr II line with  $\Delta\lambda_D = 40 \text{ mÅ}$  gives an upper limit of the non-thermal broadening (*i.e.*,  $T_{\text{kin}} = 0$ ) of  $V_{\text{nth}} \leq 3 \text{ km/s}$  through prominence D.

Assuming that the neutral lines Na D<sub>2</sub> and H $\delta$  are formed in the same prominence volume, their  $\Delta\lambda_D$  of 63 and, respectively, 150 mÅ give  $T_{\text{kin}} = 7050$  K and  $V_{\text{nth}} = 2.2$  km/s, well within the above limits. Inserting these values into Equation (1) we obtain for the Sr II line a value  $\Delta\lambda_D = 34.3$  mÅ, *i.e.*, 17% smaller than the observed  $\Delta\lambda_D = 40$  mÅ (Figure 4). Such an excess broadening was already found from our earlier observations of Fe II and Ti II lines (Wiehr *et al.*, 2013).

Similarly, we find that the observed triplet line He 3888 Å is broader than calculated for  $T_{\text{kin}} = 7050$  K and  $V_{\text{nth}} = 2.2$  km/s. This is in accordance with earlier findings of a width excess of the triplet line He 4472 Å (Stellmacher and Wiehr, 2015).

### 3.3. Marco-Shifts

The excess broadening obtained for lines from ions suggests an interaction with the magnetic field (*cf.*, Introduction). This seems to be indicated from spatial fluctuations of macro-velocities (line-shifts) relative to the mean wavelength of each spectrum. For the well documented quiet prominence D we find, consistently on both successive days, that the Sr II line shows 1.27 times larger shifts than the simultaneously observed (neutral) H $\delta$  line (Figure 5).

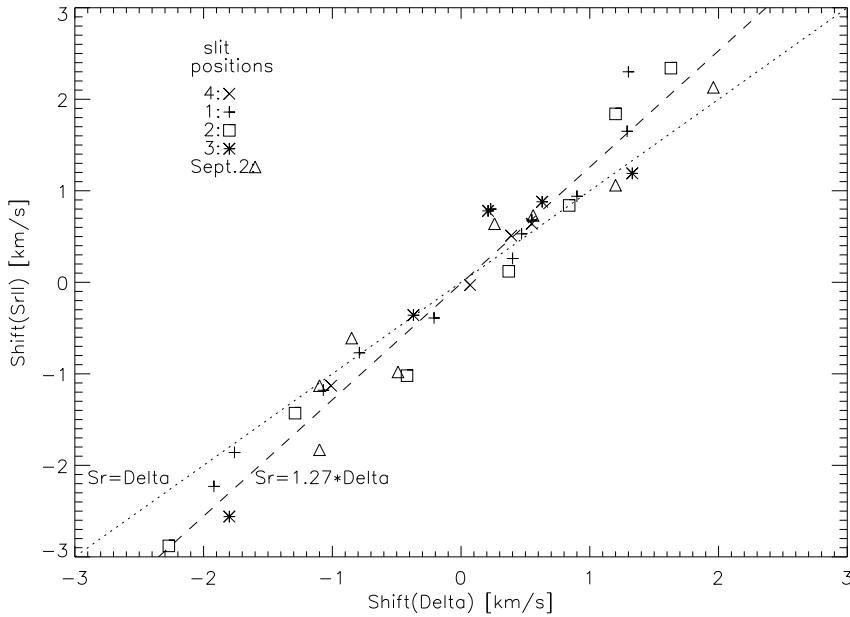


**Figure 5.** Line shifts of Sr II 4078 Å versus H $\delta$  relative to the mean wavelengths for prominence D on both days (Table 1). A linear fit gives 1.27 times higher shifts of Sr II; the dotted line denotes a 1:1-relation.

In order to verify that neutrals show equal macro-shifts (and to get an idea about the accuracy), we plot in Figure 6 shifts of the neighboring lines He I 3888



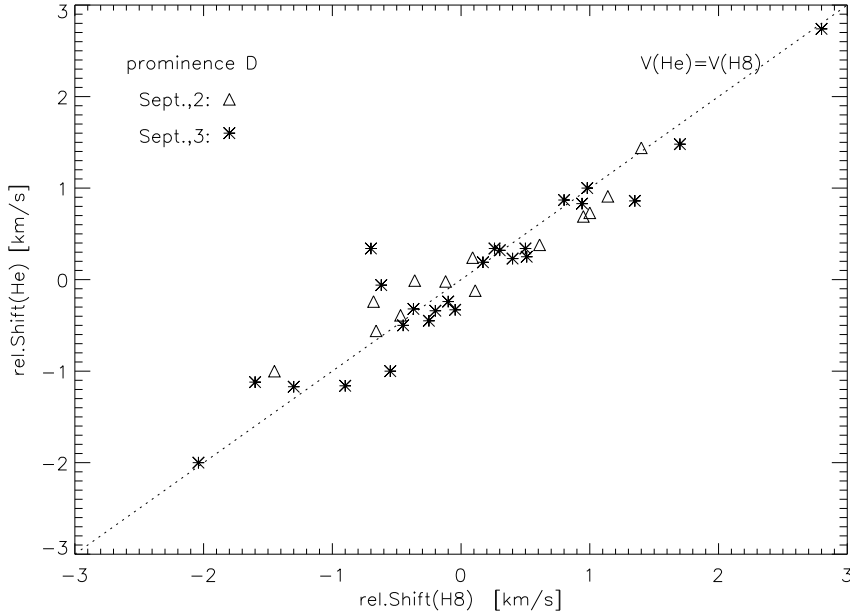


**Figure 6.** Macro-velocities from He I 3888 Å versus those from H 8 3889 Å relative to their mean wavelengths in prominence D on both days.

and H 8 3889 Å, and find a one-to-one relation with small scatter. This is equally indicated for the shifts of neutral Na and H  $\delta$ , although at larger scatter, since these lines are not simultaneously observed (*cf.*, Section 2). We check whether the shift excess of Sr II is generally valid for lines from ions using the neighboring lines Fe II 5018 Å and He I 5015 Å, earlier observed at the Locarno observatory (*cf.*, Stellmacher and Wiehr, 2015). We also find an excess shift of the (ionized) Fe II line over the (neutral) He line of the order of 1.3.

### 3.4. Unresolved Prominence Structures

The different macro-shifts of neutral and ionized lines indicate distinct emission regions. These will be of smaller scale than the spatial resolution achieved, since the spectra (of Na I and Sr II) are conspicuously similar (Figure 1). The macro-shifted spectral streaks of  $\approx 1000$  km width will result from tight bundles of superposing sub-structures. We may estimate the number of elements, responsible for the brightness of the Balmer emission within the resolution area, adopting for each of them  $E(\text{H}\alpha) = 1 \times 10^4$  erg/(s cm<sup>2</sup> ster) ( $\tau_\alpha \approx 0.1$ ; *cf.*, Stellmacher and Wiehr (2000) and references therein). The observed mean H  $\delta$  brightness of prominence D,  $E(\text{H}\delta) \leq 8 \times 10^3$  erg/(s cm<sup>2</sup> ster), corresponds in the tables by Gouttebroze *et al.* (1993) to  $\tau_\delta \leq 0.09$  and  $E(\text{H}\alpha) \leq 19 \times 10^4$  erg/(s cm<sup>2</sup> ster). The optically thin H  $\delta$  line will then originate from 19 sub-structures in the resolution area. These may readily be arranged in a single layer, if smaller than

200 km, in accordance with the narrow streaks in the spectra of prominence D, which is thus considered to fairly fulfill the conditions for Equation (1).

In contrast, the less structured spectra of the bright prominence C show much broader line widths. The nearly six times brighter H $\delta$  emission than prominence D indicates more superposed sub-structures, leading to important blending (see Gunár *et al.*, 2008), which broadens H $\delta$  and H $\gamma$  to  $\Delta\lambda_D/\lambda_0 = 4.3 \times 10^{-5}$  (as compared to prominence D with  $3.7 \times 10^{-5}$ ). Combined with the corresponding width of the Na D $_2$  line ( $\Delta\lambda_D/\lambda_0 = 1.6 \times 10^{-5}$ ), Equation (1) gives an unrealistically high thermal line broadening of  $T_{kin} = 9080$  K ( $V_{nth} = 4$  km/s) for prominence C. Its total thickness of  $\tau_\alpha \approx 25$  and the larger number of superposing sub-structures imply that the validity of Equation (1) and the deduced broadening parameters can hardly be assumed. Besides, bright prominences are rather expected to be cooler (*cf.*, Stellmacher and Wiehr, 1994a, 1994b, 1995).

#### 4. Conclusions

The similar aspects of the emission maxima of Na D $_2$  and Sr II 4078 Å (Figure 1), which have spatial widths of 2000–3000 km, suggest common emission volumes on this scale. But the ionized Sr line shows higher non-thermal line broadening and macro-shifts than the neutrals (Balmer, Na). This excess is well documented for the weaker prominence D, which is observed under good seeing conditions. In the brighter prominences (B and C) superposing structures along the line-of-sight, will smear the actual macro-shifts.

The finding of excess shifts is hardly compatible with a homogeneous (one-component) atmosphere (Terradas *et al.*, 2015). Our finding of a general shift excess of ions suggests that at smaller scales than resolved in the spectra, (*e.g.* of 150 km size), distinct volumes preferentially emit either lines from ions or from neutrals, as in the scenario of Low *et al.* (2012). Here, neutral clumps sink through the magnetic field until they are stopped when sufficiently re-ionized. Vertical motions of neutral clumps, however, cannot explain a line-of-sight velocity excess of lines from ions, which may rather be related to the stronger coupling to the magnetic field (*e.g.* Gilbert, 2011). The weak prominence field responds to the ubiquitous motions of its photospheric foot-points (Wedemeyer *et al.*, 2013; Wedemeyer and Steiner, 2014), which will induce macro-velocities. If part of these motions is converted into flows or shocks (Hillier *et al.*, 2012), additional line-shifts and non-thermal line-broadening may occur for lines from ions.

Distinct emission regions, suggested by the macro-shifts, are not in accordance with the assumption of a homogeneous prominence atmosphere as assumed in the calculations by Landman (1983, 1986) for the estimate of  $n_e$  from the observed emission ratio of Na D $_2$  and Sr II 4078 Å. An origin of Na D $_2$  and Sr II 4078 Å in different small-scale emission regions causes an uncertainty in the deduced electron density. Since the spectra of both resonance lines are conspicuously similar at the  $\approx 1000$  km scSOLA-D-17-00026.texale (see Figure 1), we estimate the influence of their distinct small-scale emission regions not to exceed the

uncertainty (20%) of deduced values, based on the different parameters (*cf.* Table 2).

The population of the upper Na I D<sub>2</sub> level,  $^2P_{3/2}$ , requires the capture of a free electron, which is furnished almost exclusively by Hydrogen;  $n_e$  then depends on the ionizing UV radiation (mainly Lyman) penetrating into the prominence. A possible dependence of the observed emission ratio on the Balmer brightness (*i.e.*, the type of the prominence, *cf.* Tables 1 and 2) is indicated for prominences A, B, C, but needs further studies. Our observations do not show significant variation of the emissions ratio (thus  $n_e$ ) over the prominence D, neither with the evolution over 24 hours, nor with height above the solar limb.

**Acknowledgments** The authors thank G. Monecke for his support with the observations. One of us (E.W.) obtained financial support by KIS.

**Disclosure of Potential Conflicts of Interest** The authors declare that they have no conflicts of interest.

## References

- Bommier, V., Landi-Degl’Innocenti, E., Leroy, J.L., Sahal-Brechot, S.: 1994, *Solar Phys.* **154**, 231 DOI10.1007/BF00681098.
- Gilbert, H.: 2011, AIP Conference Proceedings **1366**, 5 DOI10.1063/1.3625583
- Gouttebroze, P., Heinzel, P., Vial, J.-C.: 1993, *Astron. Astrophys. Suppl.* **99**, 513
- Gunár, S., Heinzel, P., Anzer, U., Schmieder, B.: 2008, *Astron. Astrophys.* **490**, 307 DOI10.1051/0004-6361:200810127
- Hillier, A., Berger, Th., Isobe, H., Shibata, K.: 2012, *Astrophys. J.* **746**, 120 DOI10.1088/0004-637X/746/2/120
- Koutchmy, S., Lebecq, Ch., Stellmacher, G.: 1983 *Astron. Astrophys.* **119**, 261
- Labrosse, P., Heinzel, P., Vial, J.-C., Kucera, T., Parenti, S., Gunár, S., Schmieder, B., Kilper, G.: 2010, *Space Sci. Rev.* **151**, 243 DOI10.1007/s11214-010-9630-6
- Labs, D., Neckel, H.: 1970, *Solar Phys.* **17**, 50
- Landman, D.A., Illing, M.E., Mongillo, M.: 1978, *Astrophys. J.* **220**, 666
- Landman, D.A.: 1983 a, *Astrophys. J.* **269**, 728
- Landman, D.A.: 1983 b, *Astrophys. J.* **270**, 265
- Landman, D.A.: 1986, *Astrophys. J.* **305**, 546
- Low, B.C., Liu, W., Berger, T., Casini, R.: 2012, *Astrophys. J.* **757**, L21 DOI10.1088/0004-637X/757/1/21
- Ramelli, R., Stellmacher, G., Wiehr, E., Bianda, M.: 2012, *Solar Phys.* **281**, 697 DOI10.1007/s11207-012-0118-2
- Shih-Huei, Y.: 1961, Publications of the Crimean Astrophysical Observatory **25**, 180
- Stellmacher, G.: 1969, *Astron. Astrophys.* **1**, 62
- Stellmacher, G., Wiehr, E.: 1994a, *Astron. Astrophys.* **286**, 302
- Stellmacher, G., Wiehr, E.: 1994b, *Astron. Astrophys.* **290**, 655
- Stellmacher, G., Wiehr, E.: 1995, *Astron. Astrophys.* **299**, 921
- Stellmacher, G., Wiehr, E.: 2000, *Solar Phys.* **196**, 357 DOI10.1023/A:1005237823016
- Stellmacher, G., Wiehr, E.: 2015, *Astron. Astrophys.* **581**, 141 DOI10.1051/0004-6361/201322781
- Terradas, J., Soler, R., Oliver, R., Ballester, J.L.: 2015, *Astrophys. J.* **802**, L28 DOI10.1088/2041-8205/802/2/L28
- Wedemeyer, S., Scullion, E., Rouppe van der Voort, L., Bosnjak, A., Antolin, P.: 2013, *Astrophys. J.* **774**, 123 DOI10.1088/0004-637X/774/2/123
- Wedemeyer, S., Steiner, O.: 2014, *Pub. Astron. Soc. Japan* **66**, 10 DOI10.1093/pasj/psu086
- Wiehr, E., Stellmacher, G., Ramelli, R., Bianda, M.: 2013, Central European Astrophysical Bulletin **37**, 487

- Wiehr, E., Stellmacher, G.: 2015, Central European Astrophysical Bulletin **39**, 35  
Wiehr, E., Stellmacher, G., Bianda, M: 2016, Central European Astrophysical Bulletin **40**, 79  
Yakovkin, N.A, Zel'dina, M.Yu. 1964, Soviet Astr. *Astron. J.* **7**, 643